

ISSN: 2281-1346



**UNIVERSITÀ DI PAVIA**  
**Department of Economics**  
**and Management**

**DEM Working Paper Series**

**Interconnected Deviations from**  
**Covered Interest Parity**

Daniel Felix Ahelegbey  
(Università di Pavia)

Oyakhilome Wallace Ibhagui  
(International Finance Corporation, USA)

**# 191 (09-20)**

Via San Felice, 5  
I-27100 Pavia

[econiaweb.unipv.it](http://econiaweb.unipv.it)

# Interconnected Deviations from Covered Interest Parity

Daniel Felix Ahelegbey<sup>a,\*</sup>, Oyakhilome Wallace Ibhagui<sup>b</sup>

<sup>a</sup>*University of Pavia, Department of Economics and Management, Italy*

<sup>b</sup>*International Finance Corporation, USA*

## Abstract

We investigate the dynamic interconnectedness among the major world cross-currency basis swap spreads during tranquil and turbulent times. We examine whether movements in the bases are merely anecdotal or provide evidence of contagion, the most central basis for spillover propagation, and implications for market participants. The result shows a high degree of interconnectedness among the bases in crisis periods with mark-to-market losses for existing exposures and large arbitrage opportunities for investors seeking new positions. We find evidence that spillovers in the bases propagate from the Euro, the Swiss franc, and the Danish krone to other bases.

*Keywords:* Covered Interest Parity, Cross-currency Basis, Currency Swaps, Dollar Funding, Financial Crisis, Interconnectedness, VAR Model.

JEL: C11, C32, F31, G01, G15,

## 1. Introduction

Over the past two decades, the global financial system has experienced several catastrophic events within and across different markets and asset classes. Among these events are: 1) the global financial crisis of 2007–2009 which was triggered by the massive defaults of sub-prime borrowers in the US mortgage market; 2) the European sovereign debt crisis of 2010–2013 which emanated from the inability of a cluster of EU member states to repay or refinance their sovereign debt and bailout heavily leveraged financial institutions without recourse to third party assistance; and 3) the ongoing distress to the world economy and global financial markets caused by the novel coronavirus pandemic in 2020. In this paper, we investigate the interconnectedness among the major funding currencies and shed some light on the new debates on the deviations from covered interest parity that has given rise the non-zero cross-currency basis swap spreads, creating arbitrage opportunities in the foreign exchange and currency derivatives markets.

The currency derivatives market constitutes a sector of financial markets that deals with the trading of financial contracts involving the exchange of currencies at a future date, and a stipulated rate. It facilitates cross-border investments and financing activities and affords agents a possibility to lessen net borrowing costs or enhance returns on lending across currencies. The cross-currency swaps market is one of the largest and most liquid currency derivative markets in the world. They are used by investors/traders as a financial instrument

---

\*Corresponding author

*Email addresses:* danielfelix.ahlegbey@unipv.it (Daniel Felix Ahelegbey), wallace@aims.ac.za (Oyakhilome Wallace Ibhagui)

for hedging currency exposure (i.e. to protect against adverse exchange rate risk) and to make extra profits (pickups) across currencies. More precisely, a cross-currency swap occurs when two parties lend and borrow an equivalent amount of money in two different currencies for a specified period (Baba and Packer, 2009a,b; Coffey et al., 2009). In this type of contract, one party lends an amount in one currency (EUR-euro) to and simultaneously borrows an equivalent amount in another currency (USD-dollars) from, the second party. The contract involves the exchange of principals (in the two different currencies) at maturity as well as an exchange of interest payments periodically until maturity in each party’s currency.

In a cross-currency swaps deal, the non-USD party (i.e. the EUR party) often seeks access to some USD. Suppose two choices are available: 1) Borrow USD directly from the cash-market; and 2) Undertake a cross-currency swap to obtain synthetic USD from the swap-market by first issuing in Euro and swapping to USD. Suppose the direct USD cost of borrowing USD directly in the cash-market is  $C$ , and the (synthetic) cost of obtaining USD in the swap-market after a cross-currency swap is  $S$ . Covered interest parity (CIP) is a theoretical condition that stipulates that the interest rates in the cash-market must correspond to that of the swap-market when both rates are expressed in the same currency, i.e., USD in this case, so that the cross-currency basis is zero/negligible/vanishingly small. The cross-currency basis swap spread, also called the “basis”, therefore measures the extent of deviations from CIP. More precisely, the basis is defined as ( $D = C - S$ ): the difference between the interest cost of the direct dollar in the cash-market and interest cost of the synthetic dollar in the swap-market. If  $D > 0$ , then the non-USD party is paying a discount to obtain synthetic USD in the swap-market while the USD party is paying a premium to the non-USD party to obtain the foreign currency. This in a way indicates the specialness of the foreign currency compared to the USD. In this case, obtaining a synthetic dollar in the swap-market is cheaper than obtaining direct USD in the cash-market. If  $D < 0$ , it is the USD funding that is more special compared to the foreign currency as it is more expensive to obtain dollar funding by swapping from the foreign currency funding than obtaining USD funding directly, which signals a willingness to pay a premium for USD. When the basis is different from zero, it creates an arbitrage opportunity that allows an agent to make riskless profits. Under the efficient market hypothesis, such an opportunity should be arbitrated away immediately by market participants but this has not been the case. Callier (1981) was the first to hint on the possibility of deviations from CIP even when the no-arbitrage models in economics and finance were most popular. This has been confirmed by a considerable number of influential studies by (Avdjiev et al. (2019); Baba and Packer (2009a,b); Coffey et al. (2009); Du and Schreger (2016); Du et al. (2018); Fong et al. (2010); Hui et al. (2011)). For instance, Du and Schreger (2016) noted that the deviations from CIP provide so much non-trivial arbitrage opportunities that exist even at a very short-horizon maturity that it poses a puzzle for the classic limits-of-arbitrage models as in Shleifer and Vishny (1997) and others that concentrate more on long-term maturity sort of market risk.

To build intuition on how the basis has evolved, Figure 1 presents the cross-currency basis swap (CCBS) vis-a-vis the USD averaged for the G-10 countries, i.e., the ten most liquid currencies of developed countries. The figure shows that between 2000–2006, the average basis swap spreads were vanishingly small and much closer to zero and the CIP rule was held approximately. The deviations in the CIP first emerged at significantly alarming levels during the global financial crisis 2007–2009. In 2010–2013, during the Eurozone crisis, the average basis swap spreads widened again albeit to a lower extent compared to the global financial crisis. Explanations for these deviations during crisis times have been attributed to

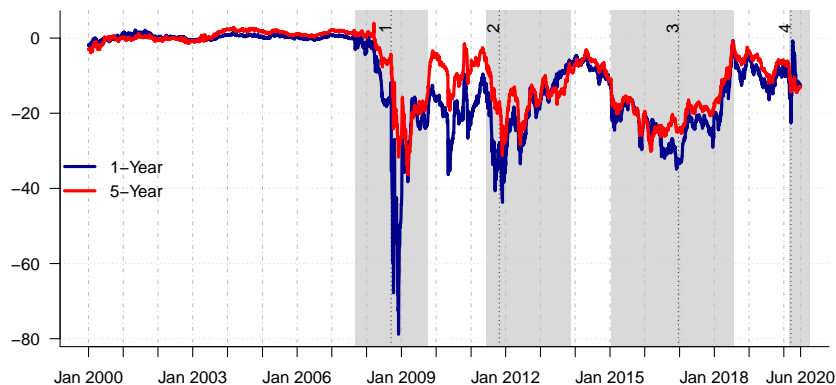


Figure 1: Averaged G-10 cross-currency basis with 1- & 5-year maturities (Jan 2000 – June 2020). Gray-shaded regions corresponds to 1) 2007–2009, 2) 2010–2013, 3) 2015–2018, and 4) 2020-1H.

the increased counterparty risk between financial institutions and the shortage of the USD, mostly because agents view the dollar as more special relative to other developed-market currencies. Such agents willingly pay a premium for the dollar while accepting a discount for the provision of their own (non-dollar) currencies in the cross-currency swap market. This action forced market participants to borrow large amounts of dollars using cross-currency swaps, thereby, worsening the deviations (see [Baba et al., 2009](#); [Baba and Packer, 2009b](#); [Baba et al., 2008](#); [Coffey et al., 2009](#); [Du et al., 2018](#); [Goldberg et al., 2011](#)). The CIP deviations narrowed slightly after the Eurozone crisis and widened again during 2015–2018. An observation, as documented by [Aizenman and Pasricha \(2010\)](#); [Avdjiev et al. \(2020\)](#); [Baba and Packer \(2009a\)](#); [Goldberg et al. \(2011\)](#), is that policy interventions of the Federal Reserve to extend dollar swap lines with global central banks narrowed the deviations after these crises. Other studies have found the post-crisis deviations to be driven by macro-financial factors, inflation differential, among other (see [Avdjiev et al., 2019](#); [Cerutti et al., 2019](#); [Ibhagui, 2019](#)).

Amid the unending CIP deviations and their continued existence, coupled with the recent pandemic-triggered financial crisis, has generated renewed debates among policymakers, and have prompted coordinated interventions from the Federal Reserve. The similar turn of events across the currency derivatives markets amidst the pandemic is a reminder that examining interconnectedness within the financial system is of crucial importance to 1) understanding the dynamics of how and from where do shocks mostly propagate; and 2) how the implications of interconnections can influence policy decisions in terms of uncovering where interventions need to be targeted, as well as the impact on financial markets, and the ultimate effect on the macroeconomy.

Our research questions are threefold. (RQ-1) Are the movements in the cross-currency basis swaps spreads merely anecdotal, or do they provide any evidence of contagion? (RQ-2) In the event of contagion, which currency is central to spillover propagation in the foreign exchange derivatives market? (RQ-3) What are the implications for financial market participants and policymakers?

To answer these questions, we formalize the derivation of interconnectedness among cross-currency basis swaps of major funding currencies via a network-based model operationalized as graphical vector autoregression (VAR). Given that data on cross-currency basis swaps, like any financial data, often exhibit contemporaneous dependencies as well as temporal lag relationships over time, the VAR model specification, therefore, accounts for the contemporaneous, serial, and cross-lagged dependencies beyond what simple stylized fact from historical

data can provide. When applying the VAR model to study relationships among variables in moderate to high dimensional multivariate time series, there are often too many parameters to estimate, compared to the available observations. A natural approach to overcome the problem of over-parametrization is via variable selection to produce parsimonious and sparse models. The introduction of networks operationalized as graphical VAR models presents a more convenient framework to achieve the parsimony/sparsity constraints while providing explainable interactions underlying the VAR model (see, e.g., [Ahelegbey et al., 2016a,b](#); [George et al., 2008](#)). Such models have in recent times been applied to infer financial contagion networks (see [Ahelegbey et al., 2016a,b](#); [Barigozzi and Brownlees, 2019](#); [Basu and Michailidis, 2015](#); [Billio et al., 2012](#); [Diebold and Yilmaz, 2014](#)). Although there are several publications on financial networks, most studies concentrate on the more traditional segment of the financial (i.e., exchange trade equities) and not on the newly emerged system of CIP deviations, which have increasingly been exploited in recent times for a more favorable investing or funding outcomes than would otherwise have been possible. Thus, this paper makes a significant contribution to the application of graphical VAR models for analyzing interconnected deviations from covered interest parity. In this study, we derive the interconnectedness among cross-currency basis swaps by adopting the Bayesian graph structural learning approach as in [Ahelegbey and Giudici \(2020\)](#).

The contribution of our work is manifold. Firstly, our study makes a significant stride in the literature on interconnected cross-currency basis swaps (CCBS). More importantly, modeling the network underlying the comovement in CCBS helps us to identify which basis is central in the widening club as well as the additional profit/loss that can be made from hedging against an adverse movement in the forex market using CCBS. Secondly, we contribute to the literature on financial networks via VAR approximated models to study interconnectedness within and across hybrids of asset classes in financial markets (see [Ahelegbey et al., 2016a](#); [Barigozzi and Hallin, 2017](#); [Billio et al., 2019, 2012](#); [Diebold and Yilmaz, 2014](#)). Thirdly, answering our research question (RQ-1) contributes to a common debate central to financial network studies on whether a densely interconnected market reduces or amplifies financial risks caused by shock events. Our contribution to this debate relates specifically to the currency derivatives markets. For the various views on the subject (see [Acemoglu et al., 2015](#); [Ahelegbey and Giudici, 2020](#); [Allen and Gale, 2000](#); [Billio et al., 2012](#); [Blume et al., 2013](#); [Freixas et al., 2000](#); [Haldane, 2013](#)).

The empirical contribution of this work studies the interconnected deviations from the covered interest parity using daily data from Bloomberg, covering between January 2000 to June 2020, and includes 25 major funding currencies (G-25) against the US dollar. Our result shows strong evidence of interconnectedness among deviations from covered interest parity for currencies both in the tranquil period and during the crisis periods (when the deviations are relatively more enlarged). We show that during crisis times (when markets are more vulnerable), the degree of interconnectedness is particularly stronger and more persistent, which implies mark-to-market losses for investors already with long basis exposures. Such events also create larger arbitrage opportunities across the currency and fixed income market for investors with US dollars seeking new positions to raise foreign currencies more cheaply by issuing in US dollars and swapping to the foreign currencies via cross-currency swaps. Central to the CIP interconnectedness is the finding that most of the spillovers propagate from the Euro, the Swiss franc, and the Danish krone bases to the other major currencies. Interestingly, the Swiss franc and the Danish krone are pegged closely to the Euro, ultimately making the most influential basis euro-centered, and the main currency that chiefly drives

contagion among the bases a Euro play.

The organization of the paper is as follows. Section 2 presents the network VAR model and discuss the Bayesian estimation. Section 3 presents a description of the data and report the results in Section 4. Section 5 concludes the paper.

## 2. Bayesian Graphical VAR Model

### 2.1. Vector Autoregressive Model

Let  $Y_t = (Y_{1,t}, \dots, Y_{n,t})$  be an  $n$ -dimensional vector of variables at time  $t$ . We consider the dynamics of  $Y_t$  as a stationary VAR( $p$ ) given by

$$Y_t = \sum_{k=1}^p B_k Y_{t-k} + U_t \quad (1)$$

$$U_t = B_0 U_t + \varepsilon_t \quad (2)$$

where  $p$  is the lag order,  $B_k$  is  $n \times n$  matrix of coefficients such that  $B_{i,j|k}$  capture the effect of  $Y_j$  on  $Y_i$  with a lag of  $k$ ,  $U_t$  is a vector of residuals independent and identically normal with covariance matrix  $\Sigma_u$ ,  $B_0$  is  $n \times n$  zero diagonal matrix such that  $B_{i,j|0}$  records the contemporaneous effect of a shock to  $Y_j$  on  $Y_i$ , and  $\varepsilon_t$  is a vector of orthogonalized disturbances with covariance matrix  $\Sigma_\varepsilon$ . From (2), the  $\Sigma_u$  can be expressed in terms of  $B_0$  and  $\Sigma_\varepsilon$  as

$$\Sigma_u = (I - B_0)^{-1} \Sigma_\varepsilon (I - B_0)^{-1'} \quad (3)$$

Equations (1) and (2) can be re-written with both contemporaneous and lagged effects as

$$Y_t = B_0 Y_t + \sum_{k=1}^p B_k Y_{t-k} - \sum_{k=1}^p B_0 B_k Y_{t-k} + \varepsilon_t \quad (4)$$

where  $B_0$  models the direct contemporaneous relationships in  $Y_t$ ,  $B_k$  captures the direct temporal effects at lag  $k$ , and  $B_0 B_k$  summarizes the indirect lagged effect via contemporaneous channels. Equation (4) is the structural VAR model, while (1) is the reduced-form VAR designed for forecasting out-of-sample observations of multiple time series. The matrices  $B_0$  and  $B_{1:p}$ , are of crucial importance to understand the dependence among elements in  $Y_t$ .

### 2.2. Network (Graphical) VAR Model

A network model is a convenient representation of the relationships among a set of variables. They are defined by nodes joined by a set of links, describing the statistical relationships between a pair of variables. The introduction of networks in VAR models helps to interpret the serial, temporal and contemporaneous relationships in a multivariate time series. To analyze (1) and (2) through networks, we assign to each coefficient  $B_{i,j|0:p}$  a latent indicator  $G_{i,j|0:p} \in \{0, 1\}$ , such that for  $i, j = 1, \dots, n$ , and  $l = 0, 1, \dots, p$ :

$$B_{i,j|l} = \begin{cases} 0 & \text{if } G_{i,j|l} = 0 \implies Y_{j,t-l} \not\rightarrow Y_{i,t} \\ \beta_{ijl} \in \mathbb{R} & \text{if } G_{i,j|l} = 1 \implies Y_{j,t-l} \rightarrow Y_{i,t} \end{cases} \quad (5)$$

where  $Y_{j,t-l} \not\rightarrow Y_{i,t}$  means that  $Y_j$  does not influence  $Y_i$  at lag  $l$ , including  $l = 0$ , which correspond to contemporaneous dependence. Following (1), (2) and (5), a network VAR

model is specified by the parameters  $(p, G_{0:p}, B_{0:p}, \Sigma_\varepsilon)$ , where  $G_{0:p}$  is related to the underlying network structure,  $B_{0:p}$  specifies the coefficients, and  $\Sigma_\varepsilon$  is the residual covariance matrix.

Let  $B^* = B_0 + \sum_{k=1}^p B_k$  and  $G^* = G_0 + \sum_{k=1}^p G_k$ . Following (5), we define two zero diagonal matrices  $A \in \{0, 1\}^{n \times n}$  and  $A^w \in \mathbb{R}^{n \times n}$ , whose  $ij$ -th element is given by:

$$A_{ij} = \begin{cases} 0, & \text{if } G_{i,j}^* = 0 \\ 1, & \text{otherwise} \end{cases}, \quad A_{ij}^w = \begin{cases} 0, & \text{if } B_{i,j}^* = 0 \\ B_{i,j}^* & \text{otherwise} \end{cases} \quad (6)$$

where  $A_{ij}$  specifies that  $Y_j \rightarrow Y_i$  exist if there is a contemporaneous or lagged directed link from  $Y_j$  to  $Y_i$ .  $A_{ij}^w$  specifies the weights of such a relationship obtained as a sum of the estimated contemporaneous and lagged coefficients. The correspondence between  $(G, B)$  and  $(A, A^w)$  is such that the former captures the short-run dynamics in  $Y_t$  while the latter can be viewed as long-term direct relationships when  $Y_t = Y_{t-1} = \dots = Y_{t-p}$ . Defining a sparse structure on  $(G, B)$  induces parsimony of the short-run model and sparsity on the long-run relationship matrices  $(A, A^w)$ .

### 2.3. Bayesian Formulation of Network VAR Models

The objective of the network model is to estimate  $(A, A^w)$  from  $(p, B_{0:p}, G_{0:p}, \Sigma_\varepsilon)$  using the available data. Estimating these parameters jointly is a challenging problem and a computationally intensive exercise. We complete the Bayesian formulation with prior specification and posterior approximation for the inference of the model parameters.

#### 2.3.1. Prior Specification

We specify the prior distributions as follows:

$$p \sim \mathcal{U}(\underline{p}, \bar{p}), \quad [B_{i,j} | G_{i,j} = 1] \sim \mathcal{N}(0, \eta), \quad G_{i,j} \sim \text{Ber}(\pi_{i,j}), \quad \Sigma_\varepsilon^{-1} \sim \mathcal{W}(\delta, S_0)$$

where  $\underline{p}$ ,  $\bar{p}$ ,  $\eta$ ,  $\pi_{i,j}$ ,  $\delta$ , and  $S_0$  are hyper-parameters. The specification for  $p$  is a discrete uniform prior on the set  $\{\underline{p}, \dots, \bar{p}\}$ ,  $\underline{p} < \bar{p}$ . The specification for  $B_{i,j}$  conditioned on  $G_{i,j}$  follows a normal distribution with zero mean and variance  $\eta$ . Thus, relevant explanatory variables with significant information to predict a response variable must be associated with coefficients different from zero and the rest (representing not-relevant variables) are restricted to zero. We consider  $G_{i,j}$  as Bernoulli distributed with  $\pi_{i,j}$  as the prior probability. Related to our specification for  $B$  and  $G$  is the stochastic search variables selection (SSVS, George et al., 2008) that assumes an indicator matrix underlying  $B$  and employs the spike and slab prior on the elements in  $B$ . The SSVS and the Bayesian graphical VAR (BGVAR, Ahelegbey et al., 2016a) have proved efficient in selecting relevant variables in over-parameterized VAR models. The difference lies in the fact that the estimated SSVS coefficient matrix often consists of elements with values significantly different from zero, whereas the rest concentrate around zero but are not ignored. Parsimony is, therefore, not guaranteed. Finally, we assume  $\Sigma_\varepsilon^{-1}$  is Wishart distributed with expectation  $\frac{1}{\delta} S_0$  and  $\delta > n$  as the degrees of freedom parameter.

In this application, we set  $\pi_{i,j} = 0.5$  which leads to uniform prior on the graph space, i.e.,  $P(G_{0:p}) \propto 1$ . Following standard application, we set  $\eta = 100$ ,  $\delta = n + 2$  and  $S_0 = \delta I_n$ .

#### 2.3.2. Posterior Approximation

Let  $Z_t = (Y_{t-1}', \dots, Y_{t-p}')'$  is  $np \times 1$  lagged observations, and denote with  $Y = (Y_1, \dots, Y_N)$  a  $N \times n$  matrix collection of all observations, and  $Z = (Z_1, \dots, Z_N)$  - a  $N \times np$  matrix collection

of lagged observations. We determine  $\hat{p}$  via a Bayesian information criterion (BIC). Under the Bayesian framework of Geiger and Heckerman (2002), the structural parameters can be integrated out analytically to obtain a marginal likelihood function over graphs. This allows us to apply an efficient Gibbs sampling algorithm to sample the graph structure in blocks (e.g., Roberts and Sahu, 1997). We approximate the graph and parameters posterior distribution via a collapsed Gibbs sampler such that for some  $\hat{p}$ , the algorithm proceeds as follows:

1. Sample via a Metropolis-within-Gibbs  $[G_0, G_{1:\hat{p}}|Y, \hat{p}]$  by
  - (a) Sampling from the marginal distribution:  $[G_{1:\hat{p}}|Y, \hat{p}]$
  - (b) Sampling from the conditional distribution:  $[G_0|Y, \hat{p}, G_{1:\hat{p}}]$
2. Sample from  $[B_0, B_{1:\hat{p}}, \Sigma_\varepsilon|Y, \hat{G}_0, \hat{G}_{1:\hat{p}}, \hat{p}]$  by iterating the following steps:
  - (a) Sample  $[B_{i,\pi_i|1:\hat{p}}|Y, \hat{G}_{1:\hat{p}}, \hat{G}_0, B_0, \Sigma_\varepsilon] \sim \mathcal{N}(\hat{B}_{i,\pi_i|1:\hat{p}}, D_{\pi_i})$  where

$$\hat{B}_{i,\pi_i|1:\hat{p}} = \sigma_{u,i}^{-2} D_{\pi_i} Z'_{\pi_i} Y_i, \quad D_{\pi_i} = (\eta^{-1} I_{d_z} + \sigma_{u,i}^{-2} Z'_{\pi_i} Z_{\pi_i})^{-1} \quad (7)$$

where  $Z_{\pi_i} \in Z$  which corresponds to  $(\hat{G}_{y_i, z_\pi|1:\hat{p}} = 1)$ ,  $\sigma_{u,i}^2$  is the  $i$ -th diagonal element of  $\hat{\Sigma}_u = (I - \hat{B}_0)^{-1} \hat{\Sigma}_\varepsilon (I - \hat{B}_0)^{-1'}$ , and  $d_z$  is the number of covariates in  $Z_{\pi_i}$ .

- (b) Sample  $[B_{i,\pi_i|0}|Y, \hat{G}_0, \hat{G}_{1:\hat{p}}, B_{1:\hat{p}}, \Sigma_\varepsilon] \sim \mathcal{N}(\hat{B}_{i,\pi_i|0}, Q_{\pi_i})$  where

$$\hat{B}_{i,\pi_i|0} = \sigma_{\varepsilon,i}^{-2} Q_{\pi_i} \hat{U}'_{\pi_i} \hat{U}_i, \quad Q_{\pi_i} = (\eta^{-1} I_{d_u} + \sigma_{\varepsilon,i}^{-2} \hat{U}'_{\pi_i} \hat{U}_{\pi_i})^{-1} \quad (8)$$

where  $\hat{U} = Y - Z \hat{B}'_{1:\hat{p}}$ ,  $\hat{U}_{\pi_i} \in \hat{U}_{-i}$  is the set of contemporaneous predictors of  $\hat{U}_i$  that corresponds to  $(\hat{G}_{y_i, y_\pi|0} = 1)$ , and  $d_u$  is the number of covariates in  $U_{\pi_i}$

- (c) Sample  $[\Sigma_\varepsilon^{-1}|Y, \hat{G}_{1:\hat{p}}, \hat{G}_0, B_{1:\hat{p}}, B_0] \sim \mathcal{W}(\delta + N, S_N)$  where

$$S_N = S_0 + (\hat{U} - \hat{U} \hat{B}'_0)' (\hat{U} - \hat{U} \hat{B}'_0) \quad (9)$$

We describe the network sampling algorithm and convergence diagnostics in Appendix Appendix A.

### 3. Data Description

Existing studies on cross-currency basis swaps (CCBS) have mostly focused on the G-10 currencies. However, recent events among countries have shown a shift in the ranking of currencies with some G-10 members gradually losing their status as a developed market currency. Prominent among such currencies is the British pound (GBP), which has traditionally been part of the G-5 currency group, however, recent events like the Brexit has turned it into a currency that can be likened to that of an emerging market. On the other hand, some emerging market currencies (e.g. the Philippine Peso<sup>1</sup>) are gradually gaining the status of a

<sup>1</sup>See <https://www.refinitiv.com/perspectives/market-insights/how-hard-has-covid-19-hit-em-currencies/> and <https://www.economist.com/asia/2020/07/23/the-philippine-peso-is-the-champion-of-emerging-market-currencies>



quasi-developed market currency given their resilience in the face of the Covid-19 pandemic. Our study on the interconnected deviations from the covered interest parity makes use of daily data from Bloomberg, covering between January 2000 to June 2020, and includes 25 major funding currencies (G-25) against the US dollar. Our G-25 consists of 13 developed and 12 emerging economies whose grouping follows the Morgan Stanley Capital International Market Classification. See Table 1 for a description of the currencies.

Market	No.	Country/Region	Currency	XCCY	Start Date	End Date
Developed	1	Euro Area	Euro	EUR	3/1/2000	6/25/2020
	2	Japan	Japanese yen	JPY	3/1/2000	6/25/2020
	3	United Kingdom	British pound	GBP	3/1/2000	6/25/2020
	4	Australia	Australian dollar	AUD	3/1/2000	6/25/2020
	5	New Zealand	New Zealand dollar	NZD	3/1/2000	6/25/2020
	6	Canada	Canadian dollar	CAD	3/1/2000	6/25/2020
	7	Denmark	Danish krone	DKK	3/1/2000	6/25/2020
	8	Switzerland	Swiss franc	CHF	3/1/2000	6/25/2020
	9	Sweden	Swedish krona	SEK	3/1/2000	6/25/2020
	10	Norway	Norwegian krone	NOK	3/1/2000	6/25/2020
	11	Israel	Israeli shekel	ILS	3/7/2011	6/25/2020
	12	Hong Kong	Hong Kong dollar	HKD	3/1/2000	6/25/2020
	13	Singapore	Singapore dollar	SGD	3/1/2000	6/25/2020
Emerging	14	Thailand	Thai baht	THB	6/26/2006	6/25/2020
	15	Malaysia	Malaysian ringgit	MYR	5/9/2005	6/25/2020
	16	Korea	Korean won	KRW	2/26/2003	6/25/2020
	17	Russia	Russian ruble	RUB	11/2/2006	6/25/2020
	18	South Africa	South African rand	ZAR	3/1/2000	6/25/2020
	19	Turkey	Turkish lira	TRY	9/19/2006	6/25/2020
	20	UAE	UAE dinar	AED	8/14/2009	6/25/2020
	21	Saudi Arabia	Saudi riyal	SAR	11/27/2009	6/25/2020
	22	Chile	Chilean peso	CLP	4/24/2009	6/25/2020
	23	Mexico	Mexican peso	MXN	2/24/2000	6/25/2020
	24	China	Chinese yuan	CNY	7/21/2009	6/24/2020
	25	Qatar	Qatari riyal	QAR	8/27/2012	12/21/2015

Table 1: The major 25 world cross-currencies grouped according to the MSCI Market Classification.

We report in Figure 2 the time series of the CCBS for the G-25 currencies grouped according to developed and emerging markets with 1- and 5-year maturities. We notice that between 2000–2006, most of the basis spreads were generally within the neighborhood of zero. This suggests that in the years preceding the global financial crisis (GFC), any CIP rule held approximately, and any deviation was quickly arbitrated away because USD was more readily available to market participants. The supply of dollar funding was hardly ever constrained, as there was the absence or diminished presence of any financial intermediation channel and neither dollar funding specialness nor foreign currency specialness existed. During the crisis of 2007–2009, the CCBS showed significant pickups in the CIP deviations most of which are negative. During this period, the supply of dollar funding was highly constrained and an intense dollar funding specialness emerged, financial intermediaries became more constrained and a strong presence of a financial intermediation channel arose.

The timeline of events shows that during the GFC, non-US entities (foreign financial institutions with interests in the US) needed USD to fund their US interests. However, these institutions were unable to have direct access to the USD cash-market because US

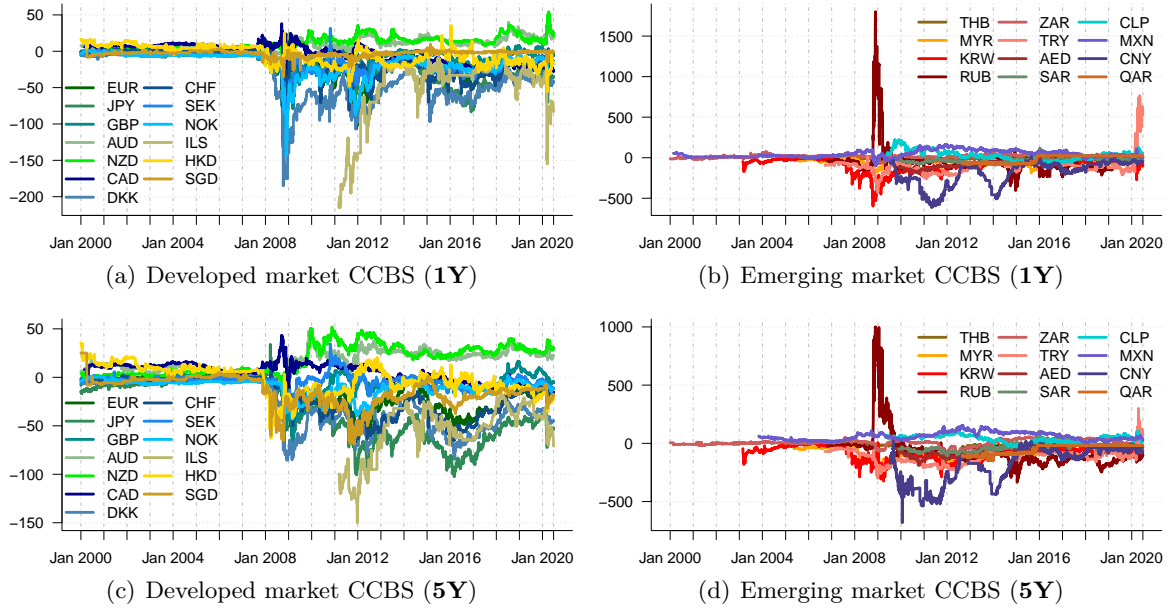


Figure 2: Time series of Cross-currency basis swaps (Jan 2000–June 2020).

financial institutions were concerned about counterparty risk. As a result, these non-US entities resorted to the cross-currency swap-market where they swapped non-USD currency to USD. This raised the cost of synthetic US dollars in the swap-market due to the high demand for dollar hedges relative to the supply of dollar hedges. The higher cost of synthetic dollars in cross-currency swap-markets forced the foreign entities to pay a premium (compared to the cost of raising direct USD in the cash-market), which led to what we know today as the cross-currency basis swap spreads. In 2010–2013, during the Eurozone crisis, the basis spreads widened again albeit to a lower extent compared to the GFC.

Table 2 presents the statistics of the basis spreads over three crisis periods: (2007–2009), (2010–2013), and first-half of 2020 (2020:1H). According to the table, the most volatile basis during the three crisis periods is usually from emerging market currencies. For both 1 and 5-year maturity basis, the Russian ruble (RUB) recorded the highest standard deviation of 321.6 between 2007–2009, the Chinese yuan (CNY) recorded the highest volatility between 2010–2013, and the Turkish lira (TRY) tops the list of the most volatile in the first half of 2020. Among the developed markets currencies, the Danish krone (DKK) was the most volatile in 2007–2009, while the Israeli shekel (ILS) tops the list between 2010–2013 and 2020:1H.

The basis can be positive or negative as seen from Figure 2 and the statistics in Table 2. Among our G-25 currencies, the majority recorded negative bases for the 1-and 5-year maturities except for the Australian dollar (AUD) and the New Zealand dollar (NZD). All these exceptions reported a positive basis spreads for 1-and 5-year maturities. According to the crisis period shown in Table 2 as well as the pre- and post-crisis periods in Figure 2, the basis for all these major currencies remained positive even when others became strongly negative. This implies that while other non-US entities were paying a premium to get (synthetic) USD in the swap-market, the AUD and NZD entities could pay a discount for the synthetic USD in the swap-market compared to the cost of direct USD in the cash-market. In other words, the USD was less special than these currencies. The Chilean peso (CLP) and the Mexican

	1-Year Maturity CCBS			5-Year Maturity CCBS		
	2007–2009	2010–2013	2020:1H	2007–2009	2010–2013	2020:1H
EUR	-21.4 ( 23.0)	-35.7 ( 19.9)	-13.7 ( 4.8)	-14.8 ( 16.2)	-29.6 ( 11.9)	-18.4 ( 4.2)
JPY	-14.2 ( 15.1)	-28.0 ( 9.4)	-35.8 ( 11.4)	-13.5 ( 20.1)	-58.5 ( 15.4)	-51.2 ( 9.1)
GBP	-20.8 ( 22.4)	-8.5 ( 7.1)	-3.3 ( 4.6)	-17.1 ( 18.1)	-7.1 ( 7.6)	-1.3 ( 4.3)
AUD	6.2 ( 9.1)	10.8 ( 6.3)	22.6 ( 7.1)	9.3 ( 11.8)	25.0 ( 6.3)	23.2 ( 2.7)
NZD	9.5 ( 5.2)	18.5 ( 5.9)	26.6 ( 12.9)	7.9 ( 8.7)	36.1 ( 6.3)	29.7 ( 4.6)
CAD	7.1 ( 7.8)	-3.6 ( 6.3)	-25.0 ( 4.3)	11.0 ( 9.4)	8.1 ( 5.0)	-15.1 ( 3.7)
DKK	-50.8 ( 47.9)	-62.5 ( 16.7)	-39.9 ( 5.5)	-30.1 ( 30.2)	-45.2 ( 10.9)	-40.3 ( 5.5)
CHF	-14.7 ( 14.3)	-28.1 ( 14.1)	-10.4 ( 5.3)	-12.8 ( 12.8)	-40.5 ( 10.2)	-16.6 ( 3.2)
SEK	-21.7 ( 21.0)	-20.5 ( 10.6)	-12.6 ( 4.0)	-7.2 ( 7.9)	0.4 ( 8.6)	-7.3 ( 2.9)
NOK	-25.8 ( 25.3)	-32.0 ( 17.2)	-12.8 ( 3.6)	-14.8 ( 12.3)	-19.0 ( 9.3)	-9.5 ( 2.8)
ILS	0.0 ( 0.0)	-62.4 ( 65.3)	-66.6 ( 27.5)	0.0 ( 0.0)	-57.0 ( 45.3)	-49.7 (11.4)
HKD	-4.6 ( 10.0)	-15.2 ( 10.0)	-22.9 ( 8.9)	-15.3 ( 18.0)	-5.3 ( 12.3)	-21.9 ( 5.2)
SGD	-6.9 ( 5.1)	-5.5 ( 2.8)	-1.8 ( 3.1)	-19.6 ( 15.9)	-29.8 ( 13.0)	-17.4 ( 6.8)
THB	-12.1 ( 13.2)	-17.0 ( 8.4)	-3.9 ( 2.3)	-9.8 ( 12.6)	-71.2 ( 41.9)	-23.6 (15.2)
MYR	-57.4 ( 51.7)	-74.9 ( 30.6)	-83.1 ( 25.5)	-95.2 ( 61.3)	-115.8 ( 29.9)	-86.4 (30.0)
KRW	-201.8 (115.3)	-120.3 ( 45.3)	-93.7 ( 41.7)	-114.2 ( 74.0)	-127.0 ( 43.0)	-91.6 (26.5)
RUB	62.0 (321.6)	-68.3 ( 33.6)	-48.0 ( 9.7)	117.8 (252.8)	-81.6 ( 36.3)	-117.7 (14.2)
ZAR	9.5 ( 27.9)	13.7 ( 15.2)	-9.0 ( 12.7)	4.7 ( 26.8)	-20.8 ( 31.9)	-28.5 (20.6)
TRY	-120.6 ( 71.4)	-146.6 ( 62.1)	235.9 (293.5)	-115.0 ( 63.4)	-165.3 ( 39.8)	0.9 (90.4)
AED	-3.7 ( 20.7)	-107.2 ( 39.7)	-26.9 ( 12.1)	-6.5 ( 17.7)	-94.6 ( 33.3)	-31.2 (15.8)
SAR	-1.2 ( 6.5)	-50.5 ( 12.4)	-39.0 ( 8.7)	-1.6 ( 8.8)	-64.0 ( 17.1)	-50.7 (18.8)
CLP	26.5 ( 60.4)	61.8 ( 46.9)	49.7 ( 28.6)	12.0 ( 22.7)	60.2 ( 16.7)	44.6 (28.0)
MXN	29.7 ( 38.5)	103.7 ( 30.0)	31.7 ( 22.4)	53.0 ( 22.4)	90.5 ( 31.5)	45.5 ( 9.1)
CNY	-24.4 ( 67.8)	-315.3 (149.6)	-47.3 ( 11.4)	-36.7 ( 96.0)	-321.4 (125.3)	-55.1 (19.1)
QAR	0.0 ( 0.0)	-24.4 ( 34.2)	24.7 ( 0.1)	0.0 ( 0.0)	-36.6 ( 51.4)	-19.0 ( 0.0)

Table 2: Statistics of the CCBS in mean and standard deviations (in parenthesis).

peso (MXN) appear positive, but it should be noted that their bases are quoted on the dollar leg as is conventional in the market for these currencies rather than the non-dollar leg as is normally the case with other currencies. Thus, even though they seem positive, they are more in the class of negative basis currencies when their bases are quoted on the non-dollar leg as is common in the swap-market, and hence do not belong to the class of the well known positive basis currencies, i.e. AUD and NZD.

Let  $C_{i,t}$  denote the daily CCBS of country  $i$  at time  $t$ . We compute daily changes in the basis by a difference in the successive daily CCBS,  $Y_{i,t} = \Delta C_{i,t} = (C_{i,t} - C_{i,t-1})$ . Table 3 reports a set of summary statistics for the daily changes in the CCBS with 1 and 5-year maturities for the full sample between January 2000 to June 2020. We reported the mean (scaled by 100), standard deviation, skewness, and excess kurtosis. From the summary statistics, we notice that the daily changes in the 1-year basis have a zero mean and a relatively high standard deviation, which ranges between 0.99 (New Zealand dollar - NZD) and 3.80 (Israeli shekel - ILS) for developed markets, and between 1.41 (Thai baht - THB) and 24.63 (Russian ruble - RUB) for emerging markets. The highest standard deviations are those of Russia (RUB) and Turkey (TRY). The skewness of the daily changes in the 1-year basis ranges between -26.61 (Israeli shekel - ILS) and 6.87 (Turkish lira - TRY) with the majority being negative. The excess kurtosis varies between 18.63 (South African rand - ZAR) and 1523.39 (Israeli shekel - ILS). The daily changes in the 5-year CCBS also show a zero mean and a relatively high standard deviation, which ranges between 0.63 (Swedish krona - SEK)

Stats	1-Year Maturity CCBS				5-Year Maturity CCBS			
	Mean	Sdev	Skew	Kurt	Mean	Sdev	Skew	Ex-Kurt
EUR	-0.18	1.94	-1.53	122.53	-0.31	0.90	-0.26	33.83
JPY	-0.51	1.65	-0.20	57.55	-0.61	1.07	0.03	45.78
GBP	0.03	1.69	-3.19	161.40	0.06	0.76	0.30	35.56
AUD	0.18	1.19	0.83	226.43	0.25	1.10	-0.67	128.65
NZD	0.41	0.99	0.08	39.03	0.40	0.82	0.36	35.95
CAD	-0.43	1.11	-2.06	64.96	-0.24	0.95	-22.50	1226.67
DKK	-0.58	2.24	-3.04	128.41	-0.63	1.24	-2.60	98.36
CHF	-0.20	1.70	1.07	88.08	-0.29	0.89	0.20	47.40
SEK	-0.23	1.20	-1.64	44.31	-0.11	0.63	2.41	61.32
NOK	-0.19	1.41	-6.37	386.06	-0.12	0.65	-0.33	82.12
ILS	-1.33	3.80	-26.61	1523.39	-1.14	2.12	-17.09	821.87
HKD	-0.51	1.61	0.80	28.98	-0.92	1.28	-0.92	28.21
SGD	-0.01	1.24	-0.61	123.98	-0.70	1.26	-3.91	109.64
THB	-0.05	1.41	-1.41	87.32	-0.24	2.41	-0.88	52.14
MYR	-1.33	4.96	4.59	162.28	-1.37	3.37	-0.20	26.19
KRW	-1.43	7.72	-1.91	60.39	-1.56	6.63	-1.40	27.51
RUB	-0.64	24.63	1.94	195.94	-1.72	20.27	-3.87	245.73
ZAR	0.27	3.26	0.18	18.63	-0.67	2.49	0.20	30.66
TRY	8.58	12.67	6.87	207.79	1.16	7.89	1.39	176.38
AED	-0.42	3.32	-7.68	293.58	-0.59	3.32	-0.82	40.96
SAR	-0.58	3.68	0.32	47.92	-0.95	4.51	0.42	31.90
CLP	0.82	4.94	1.75	87.02	0.55	2.28	2.18	61.03
MXN	0.08	4.60	-1.00	91.95	0.42	2.69	1.68	166.15
CNY	-0.87	7.82	-3.86	97.76	-1.19	11.00	-1.06	129.30
QAR	0.43	1.87	-7.99	393.69	-0.30	4.41	-2.81	161.37

Table 3: Summary statistics of daily changes in cross-currency basis swaps (Jan 2000–June 2020).

and 20.27 (Russian ruble - RUB). The second most volatile basis after the Russian ruble (RUB) is the Chinese yuan (CNY). The skewness of the daily changes in the 5-year CCBS ranges between -22.25 (Canadian dollar - CAD) and 2.41 (Swedish krona - SEK) with the majority being negative. The excess kurtosis varies between 26.19 (Malaysian ringgit - MYR) and 1226.67 (Canadian dollar 10 - CAD). Thus, the daily changes in the 1 and 5-year CCBS indicate a leptokurtic behavior.

#### 4. Empirical Findings and Discussion

We apply our proposed estimation methodology to study the dynamics of interconnectedness among the G-25 CCBS via a yearly (approximately 240 trading days) rolling window. Our choice of window size is to capture the annual (12-months) dependence among the basis. We set the increments between successive rolling windows to one month. The first window covers February 2000 – January 2001, followed by March 2000 – February 2001, and the last from July 2019 – June 2020. In total, we have 234 rolling windows. We examine the dynamics of the basis interconnectedness via network measures based on density and turbulence index. We summarize the network topology via network centrality measures.

We select the appropriate lag of the VAR via a Bayesian information criterion (BIC) for different lag orders ( $p \in \{1, \dots, 7\}$ ). Table 4 presents the BIC scores for the lag order selection exercise. The minimum BIC score which indicates the optimal lag order is represented in boldface. Thus, we conduct our rolling estimations using a lag order  $p = 1$ .

p	1	2	3	4	5	6	7
BIC (1Y)	<b>48.15</b>	48.27	48.58	48.96	49.30	49.65	50.10
BIC (5Y)	<b>35.79</b>	36.25	36.75	37.30	37.89	38.51	39.11

Table 4: The BIC for lag order selection. Boldface values indicate the minimum BIC.

#### 4.1. Network Density and Financial Turbulence

Here we address our first research question: (RQ-1) Are the movements in the cross-currency basis swaps spreads merely anecdotal, or do they provide any evidence of contagion?

We characterize through numerical summaries the dynamic interconnectedness among the G-25 by monitoring the network density and turbulence index. Let  $A$  be an  $n$ -node unweighted adjacency matrix without self-loop. The network density is given by the number of links in the estimated network divided by the total number of possible links.

Let  $Y = (Y_1, \dots, Y_n)$  be  $n$  vector of daily change in the basis with standard deviations  $\sigma(Y) = (\sigma_1, \dots, \sigma_n)$ . Suppose  $\Omega = (I + A^w)'(I + A^w)$  is their constrained partial correlations matrix. Following [Ahegbey and Giudici \(2020\)](#) and [Kritzman and Li \(2010\)](#), we compute the network-based turbulence index ( $T^{sys}$ ) as

$$T^{sys} = \sqrt{\frac{1}{n} \sigma(Y)' \Omega \sigma(Y)} \quad (10)$$

where  $T^{sys}$  captures the average degree of unusual changes in asset returns and their interactions. The turbulence index signals wide spread market turmoil and can be viewed as a measure of market-level fears composed by asset volatilities that are amplified through interconnectedness.

Figure 3 shows the time series of the turbulence index and network density for the cross-currency basis at the 1-year and 5-year maturity. Across both maturities, there is striking evidence that the network density and turbulence index are congruent in behavior. That is, the result shows strong evidence of a spike in interconnectedness among deviations from CIP during the global financial crisis (GFC), through the European sovereign crisis (ESC), the oil crisis of 2014–2016, tax reform shock of late-2017 – mid-2018, and in the heat of the COVID pandemic. The severity of turmoil in the foreign exchange currency derivatives market tracked by the turbulence index recorded its historical highest spike during the 2007–2009 global financial crisis, and moderate spikes during the oil crisis and the recent Covid-19 pandemic. Although the severity of the turmoil in the currency derivatives market was much higher during the GFC compared to the Covid-19 period, the degree of interconnectedness during the latter is much greater than the former. So, therefore, if the turbulence seen in the market during the COVID pandemic was not taken serious and allowed to continue, then the devastating consequences in the foreign derivatives market would have been much larger than was ever seen, even trumping worst of the global financial crisis.

The figure shows that market network density as a result of the COVID-19 induced sell-off is much greater than any period of market crisis in the last 20 years, and this include the period of GFC when the deviations from CIP first emerged with the most vengeance. As would normally be expected, we also find that market turbulence, typified by fear and panic, intensified in foreign exchange derivatives markets in all the crisis times. An especially important outcome of our findings is that the subsequent damage or pressure in this market would have been more lethal or severe during the recent Covid-19 sell-off in the absence of

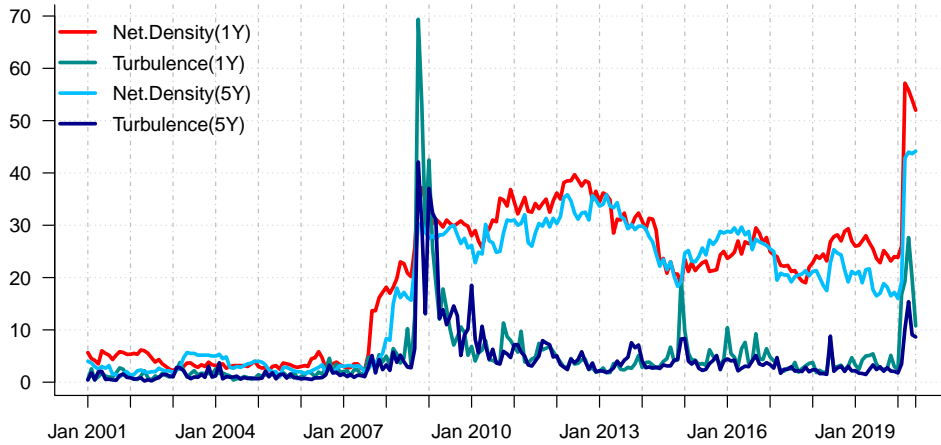


Figure 3: Network Density and Turbulence Index among CCBS with 1 & 5-year maturities.

the coordinated market intervention by the Federal Reserves via large liquidity provisions and new swap lifelines.

From Figure 3, the behavior of the network density and turbulence index during the GFC are strikingly similar to the behavior exhibited most recently at the height of the Coronavirus pandemic in 2020-1H. The spikes in both indices at the onset of both crisis periods indicate elevated levels of unusualness in the foreign currency derivatives markets, a rise in volatility, and co-movement among cross-currency basis. Just as in the GFC, this unusualness manifested as a decoupling of previously held relations. During the GFC, it manifested as the emergence of significant deviations from covered interest parity, which continued post-GFC as a wider (non zero) cross-currency basis swap spread. In the recent COVID pandemic, however, it is exhibited as an increase in uncertainty that manifests in wider cross-currency basis swap spreads, as the unusualness caused by anticipated dollar stress mounts in the foreign exchange derivative markets. As in the GFC, one potential reason for the unusualness that results from this pressure in the foreign currency derivatives market is partly due to fear of dollar liquidity shortages (supply-side) and an increase in safe asset demand (demand-side), both of which led to the wider cross-currency basis seen at the height of the pandemic in 2020-H1. It was in response to these concerns that the Federal Reserve increased existing swap lines and entered new swap lines with other countries to ease these pressures.

In the interest to address whether the movements in the basis swap spreads provide evidence of contagion, Figure 4 shows a plot comparing the average cross-currency basis against Net-Density and Turbulence index. The figure shows that the more negative the average cross-currency basis swap spreads the higher the significant rise in the market network density and turbulence. This suggest a strong evidence of contagion in all the identified crisis periods, and did not occur in the same magnitude during the more tranquil times in the foreign exchange derivatives market. Table 5 confirms the negative relationship between the movements in the cross-currency basis swap spreads and the market network density and turbulence through a cross-correlation analysis. From the table, the most significant cross-correlation of the average cross-currency basis swap spreads (Av.CCBS) with the network density and turbulence occurs at lag 0 for the 1-year maturity and lag 1 for the 5-year maturity. The network density and turbulence index for both maturities, however, exhibit a positive contemporaneous relationship. Thus, the evidence indicates that periods of very

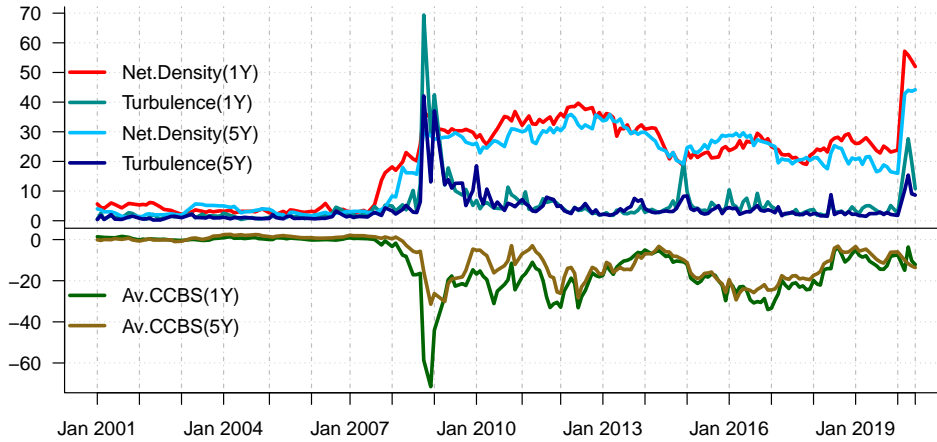


Figure 4: **Network Density, Turbulence Index and Average Cross-Currency Basis.** This figure plots the monthly average cross-currency basis swaps, the degree of interconnectedness and turbulence index between January 2001 and June 2020.

$x_{t+h}$	-4	-3	-2	-1	0	1	2	3	4
Cross Correlation of $\Delta$ Net.Density (1Y) with									
$\Delta$ Av.CCBS (1Y)	0.023	-0.020	0.065	0.066	<b>-0.312</b>	-0.008	0.030	0.053	0.033
Cross Correlation of $\Delta$ Turbulence (1Y) with									
$\Delta$ Av.CCBS (1Y)	-0.011	0.129	-0.067	0.131	<b>-0.315</b>	-0.302	0.105	0.137	0.024
Cross Correlation of $\Delta$ Turbulence (1Y) with									
$\Delta$ Net.Density (1Y)	0.036	-0.200	-0.054	0.062	<b>0.318</b>	0.048	-0.090	0.027	-0.035
Cross Correlation of $\Delta$ Net.Density (5Y) with									
$\Delta$ Av.CCBS (5Y)	-0.079	-0.058	-0.017	0.125	-0.109	<b>-0.189</b>	-0.150	-0.005	0.014
Cross Correlation of $\Delta$ Turbulence (5Y) with									
$\Delta$ Av.CCBS (5Y)	0.021	0.025	0.066	-0.068	0.120	<b>-0.425</b>	0.124	-0.084	0.035
Cross Correlation of $\Delta$ Turbulence (5Y) with									
$\Delta$ Net.Density (5Y)	-0.079	-0.007	-0.086	0.016	<b>0.254</b>	0.012	-0.046	0.013	0.011

Table 5: Cross Correlation of average daily basis, network density and turbulence index for both maturities. The result shows the correlation of  $x_{t+h}$  (the row variable) with  $y_t$  (the column variable). Boldface values indicate the significant correlations.

high negative deviations in CIP are often associated with a high degree of interconnectedness and turbulence in foreign exchange derivatives markets.

Based on the similarity in the behaviors of the network density and turbulence index, two stylized facts can emerge: 1) The behavior of the cross-currency basis swap spreads in the foreign exchange derivatives markets during the pandemic is in several ways more similar to the GFC than it is to other periods of stress. Just like during the GFC, it appears that the foreign exchange derivative market is in a transition to a quieter period where stress is diminished in the market, dollar funding pressure is lowered and deviations from CIP is less acute; and 2) Based on the behavior of the network density and turbulence index during

the GFC, the subsequent pattern in the foreign exchange derivatives market after the recent pandemic could be one where there is diminished unusualness, turbulence is quietened, and deviations from CIP become less pronounced, i.e. the basis becomes much less negative (tighter), especially given the bazooka of liquidity that the Federal Reserve has embarked upon, weakening implications this has for the US dollar and the enhancement of cross border flows. This is a well-known triangular relationship documented in [Avdjiev et al. \(2019\)](#) where it is shown that a weaker dollar goes with an increased banking flow (i.e. supply of US dollars in the foreign exchange derivatives markets) and a tighter cross-currency basis swap spread.

#### 4.2. Network Topology and Centrality

We now turn our attention to the second research question: (RQ-2) In the event of contagion, which basis swap spreads is central to spillover propagation in the foreign exchange derivatives market?

To address the above question, we first begin by characterizing the dynamic interconnectedness in the covered interest parity, monitoring the topological structure of the G-25 cross-currency basis swaps, and an assessment of the most critical (or central) basis to the foreign exchange derivatives market. We briefly present the metric for the construction of the network topology and some standard network centrality measures used in this study.

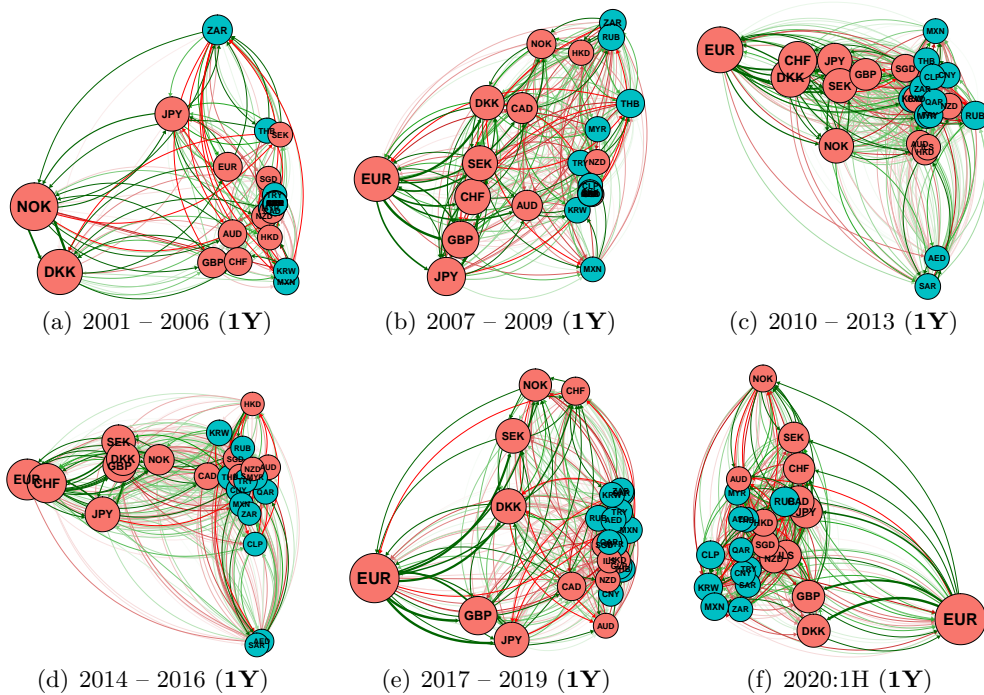


Figure 5: Networks of CCBS with **1-year** maturity. Red links denote negative effects and green for positive interactions. Red (green) nodes are developed (emerging) market currencies.

Node centrality in networks addresses the questions of how important a node/variable is in the network. Commonly discussed centrality measures include in-degree (number of in-bound links), out-degree (number of out-bound links), authority, and hub scores. The authority score of node- $i$  is a weighted sum of the power/hub score of the vertices with directed links towards node- $i$ . The hub score of node- $j$  is the weighted sum of the power/authority score of



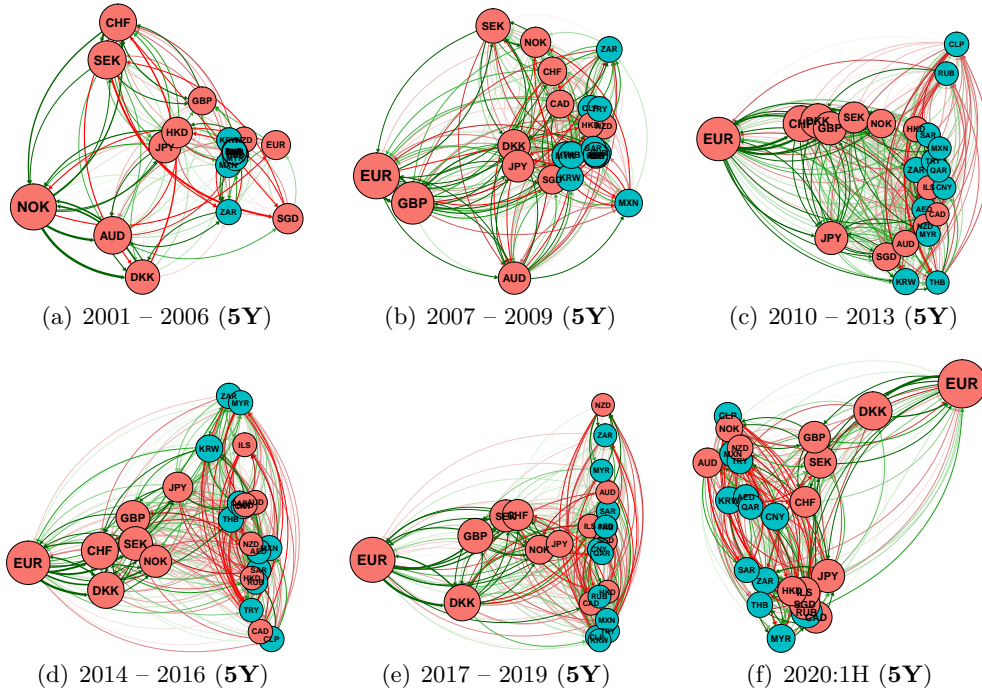


Figure 6: Networks of CCBS with **5-year** maturity. Red links denote negative effects and green for positive interactions. Red (green) nodes are developed (emerging) market currencies.

vertices with a directed link from node- $j$ . The authority and hub scores can be obtained via eigendecomposition of  $(AA')$  and  $(A'A)$ . The absolute value of the eigenvectors associated with the largest eigenvalue is usually used as the authority and hub centrality score. A hub node usually has a large out-degree and authority has a large in-degree. From a financial viewpoint, nodes with high authority scores/in-degree are highly influenced by others, while high hub scores/out-degree nodes are the influencers.

We report in Figures 5 and 6 the topological structure interconnectedness of 1-year and 5-year maturity basis over six time periods: (2000–2006), (2007–2009), (2010–2013), (2014–2016), (2017–2019), and (2020:1H). Network links are color-coded with red-links indicating a negative effect and green-links mean positively weighted edges. The nodes are also color-coded such that red-nodes represent developed market currencies and green-nodes are for emerging markets. The size of the nodes is proportional to their hub scores.

The network topology shows evidence of clustering behavior among the currencies. More importantly, the red-color nodes (the developed market currencies) seem to move together due to similarities in underlying basis conditions. Likewise, the green-color nodes (the emerging market currencies) also tend to move together due to similarities in underlying conditions. Except for 2001–2006 network which has NOK (Norwegian krone) and the DKK (Danish krone) as the biggest sized nodes (i.e., the most influential), the rest of the sub-period networks show EUR (the Euro) as the largest-sized node (i.e., the most influential).

In the interest of finding the most influential cross-currency basis, Table 6 reports the summary of the centrality ranking of the most influential currencies over the sub-periods and full sample based on the median statistics of the hub and authority scores. The table shows the top three most influential currencies for the sub-periods, and the full sample ranking

	Rank	1-Year Maturity CCBS		5-Year Maturity CCBS	
		Hub	Auth	Hub	Auth
Sub-Periods: Top Three Most Influential Currencies					
2001 – 2006	1	ZAR ( 0.423 )	JPY ( 0.267 )	SEK ( 0.243 )	NOK ( 0.243 )
	2	HKD ( 0.291 )	KRW ( 0.244 )	HKD ( 0.219 )	AUD ( 0.200 )
	3	NOK ( 0.264 )	ZAR ( 0.239 )	AUD ( 0.176 )	ZAR ( 0.181 )
2007 – 2009	1	JPY ( 0.291 )	JPY ( 0.274 )	JPY ( 0.279 )	JPY ( 0.277 )
	2	EUR ( 0.286 )	DKK ( 0.253 )	CAD ( 0.242 )	DKK ( 0.269 )
	3	DKK ( 0.251 )	MXN ( 0.247 )	GBP ( 0.238 )	SGD ( 0.258 )
2010 – 2013	1	EUR ( 0.269 )	SEK ( 0.272 )	EUR ( 0.277 )	EUR ( 0.297 )
	2	CHF ( 0.256 )	EUR ( 0.255 )	SEK ( 0.266 )	JPY ( 0.254 )
	3	SEK ( 0.255 )	JPY ( 0.251 )	JPY ( 0.225 )	CHF ( 0.237 )
2014 – 2016	1	CHF ( 0.282 )	JPY ( 0.273 )	EUR ( 0.252 )	KRW ( 0.251 )
	2	JPY ( 0.249 )	CLP ( 0.248 )	ZAR ( 0.249 )	EUR ( 0.249 )
	3	EUR ( 0.232 )	SEK ( 0.218 )	CNY ( 0.245 )	RUB ( 0.238 )
2017 – 2019	1	EUR ( 0.304 )	EUR ( 0.306 )	EUR ( 0.293 )	DKK ( 0.277 )
	2	DKK ( 0.299 )	CHF ( 0.295 )	DKK ( 0.268 )	GBP ( 0.257 )
	3	CHF ( 0.260 )	DKK ( 0.282 )	GBP ( 0.264 )	EUR ( 0.243 )
2020:1H	1	KRW ( 0.247 )	JPY ( 0.262 )	KRW ( 0.315 )	ZAR ( 0.267 )
	2	EUR ( 0.245 )	KRW ( 0.251 )	JPY ( 0.273 )	TRY ( 0.253 )
	3	GBP ( 0.239 )	NOK ( 0.248 )	AUD ( 0.270 )	JPY ( 0.252 )
Full-Sample: All G-25 Currencies					
Core	1	EUR ( 0.253 )	JPY ( 0.260 )	EUR ( 0.229 )	JPY ( 0.223 )
	2	DKK ( 0.243 )	NOK ( 0.238 )	CHF ( 0.219 )	EUR ( 0.221 )
	3	CHF ( 0.239 )	SEK ( 0.227 )	JPY ( 0.211 )	CHF ( 0.218 )
	4	JPY ( 0.227 )	DKK ( 0.220 )	DKK ( 0.197 )	KRW ( 0.216 )
	5	ZAR ( 0.220 )	EUR ( 0.219 )	SEK ( 0.192 )	GBP ( 0.212 )
Semi-Periphery	6	NOK ( 0.216 )	KRW ( 0.216 )	KRW ( 0.190 )	ZAR ( 0.203 )
	7	SEK ( 0.210 )	GBP ( 0.213 )	ZAR ( 0.189 )	DKK ( 0.193 )
	8	GBP ( 0.207 )	CHF ( 0.204 )	MYR ( 0.184 )	SEK ( 0.171 )
	9	HKD ( 0.192 )	ZAR ( 0.188 )	GBP ( 0.171 )	NOK ( 0.169 )
	10	MXN ( 0.187 )	HKD ( 0.176 )	HKD ( 0.169 )	HKD ( 0.157 )
	11	KRW ( 0.178 )	MXN ( 0.167 )	AUD ( 0.164 )	MYR ( 0.157 )
	12	RUB ( 0.169 )	RUB ( 0.155 )	RUB ( 0.154 )	RUB ( 0.155 )
	13	MYR ( 0.154 )	AUD ( 0.151 )	THB ( 0.148 )	THB ( 0.151 )
	14	THB ( 0.128 )	CAD ( 0.148 )	MXN ( 0.130 )	MXN ( 0.150 )
	15	CAD ( 0.124 )	MYR ( 0.144 )	NOK ( 0.121 )	CLP ( 0.145 )
Periphery	16	AUD ( 0.123 )	THB ( 0.126 )	TRY ( 0.121 )	SGD ( 0.142 )
	17	TRY ( 0.114 )	NZD ( 0.117 )	CLP ( 0.121 )	AUD ( 0.137 )
	18	SGD ( 0.104 )	TRY ( 0.113 )	SGD ( 0.120 )	TRY ( 0.131 )
	19	SAR ( 0.103 )	CNY ( 0.096 )	SAR ( 0.115 )	AED ( 0.114 )
	20	NZD ( 0.101 )	SGD ( 0.078 )	NZD ( 0.093 )	CAD ( 0.106 )
	21	CLP ( 0.071 )	SAR ( 0.077 )	CAD ( 0.092 )	NZD ( 0.099 )
	22	CNY ( 0.071 )	AED ( 0.051 )	AED ( 0.084 )	SAR ( 0.090 )
	23	AED ( 0.049 )	CLP ( 0.044 )	CNY ( 0.075 )	CNY ( 0.067 )
	24	ILS ( 0.000 )	ILS ( 0.000 )	ILS ( 0.000 )	ILS ( 0.000 )
	25	QAR ( 0.000 )	QAR ( 0.000 )	QAR ( 0.000 )	QAR ( 0.000 )

Table 6: Centrality ranking 1-year and 5-year swaps of according to hub and authority score.

from “core” (1st to 5th), through “semi-periphery” (6th to 15th), to “periphery” (16th to 25th). The result shows that central to the network of interconnectedness for spillovers and propagation of contagion is the Euro with the highest hub score for both 1-year and 5-year maturity bases. The Japanese yen (JPY) is the most central in terms of authority score for both 1-year and 5-year maturity bases.

Over the full sample, the most influential (in terms of hub score ranking) currency for spillovers and propagation is the Euro. It is usually within the top three highest hub-score currency over the various sub-periods. The next most influential 1-year maturity basis is the Danish krone (DKK), followed by the Swiss franc (CHF), the Japanese yen (JPY), and the South African rand (ZAR). The next most influential 5-year maturity basis after the Euro according to the full sample statistics is the Swiss franc (CHF), followed by the Japanese yen (JPY), the Danish krone (DKK), and the Swedish krona (SEK). A surprise finding from the hub ranking is the South African rand - ranked 5th for the 1-year maturity, and 7th highest hub score for the 5-year maturity.

The summary ranking of the authority scores for the 1-year maturity shows that the top 5 basis is the Japanese yen (JPY), the Norwegian krone (NOK), the Swedish krona (SEK), the Danish krone (DKK), and the Euro. The top 5 authority scores for the 5-year maturity are the Japanese yen (JPY), the Euro, the Swiss franc (CHF), the Korean won (KRW), and the British pound (GBP). Another surprise finding from the authority ranking is the Korean won - ranked 6th for the 1-year maturity, and 4th highest authority score for the 5-year maturity.

Overall, the result shows that central to the CIP interconnectedness is the finding that most of the spillovers propagate from the Euro, the Swiss franc, and the Danish krone bases to the other major currencies. Interestingly, the Swiss franc and the Danish krone are pegged closely to the Euro, ultimately making the most influential basis Euro-centered. This suggests that shocks that impair the functioning of the global cross-currency basis swap-markets first manifest in the Euro currency basis before spreading to others, making the Euro cross-currency basis swap to have the most influence on the variability of the bases of other major currencies. One plausible reason, we believe, is that the euro-dollar pair, and by extension its associated basis, being the most liquid in the world, partly explains this phenomenon. The euro basis viz-a-viz the dollar is the most actively traded cross-currency basis swaps in the global derivatives market.

#### *4.3. Implication For Market Participants*

Here we address our third and final research question: (RQ-3) What are the implications for financial market participants and policymakers?

The result shows that shocks in the global cross-currency basis swap-markets first manifest in the euro currency swap-markets before spreading to others, making the euro cross-currency basis swap to have the most influence on the variability of the bases of other major currencies. One plausible reason, we believe, is that the euro-dollar pair, and by extension its associated basis, being the most liquid in the world, partly explains this phenomenon. The euro basis viz-a-viz the dollar is the most actively traded cross-currency basis swaps in the global derivatives market. One implication of our finding is that financial market participants need to track events in the euro basis (together with the bases of other currencies pegged/linked closely to it) much more carefully than before. This is because the euro basis is central to contagion in the cross-currency swap-markets, and sets the stage for the dynamics observed on the other basis swap spreads. It can, therefore, not be excluded from empirical and theoretical modeling of the cross-currency swap-markets. Apart from providing a benchmark in the market, the

euro basis is the most liquid basis swap spread, accounting for a large number of trading volumes and has shown to have the most tactical influence on the other basis swap spreads.

For agents with exposure to the foreign exchange derivatives markets, there are several financial market implications of the stylized facts derived from the above findings. First, for dollar entities who look to enter new hedges against exchange rate risk for their foreign currency exposure, it is less expensive and more cost-effective to do those hedges before the cross-currency basis associated with their intended currencies of exposure becomes tighter. This will help to minimize basis risk and enhance marked-to-market gains from upward movements (subsequent tightening) in the basis. In this case, one potentially profitable arbitrage trade when the basis is more negative (and before the basis becomes tighter or less negative) would be to borrow in the currency with a higher interest rate (i.e. US dollar) and lend in the currency with a lower interest rate that has a negative basis (i.e. Euro), with exposure to foreign exchange risk well hedged. This is the opposite of the traditional carry trade. Second, the same is true for borrowers of these foreign currencies who first borrow US dollars before entering a foreign exchange derivatives contract of swapping USD to their foreign currencies of choice as it is potentially cheaper for such entities to achieve this when the cross-currency basis is wider and before it becomes tighter as would be expected from the stylized fact. In this way, these foreign currencies can be raised more cheaply.

For currencies with a positive basis, the advantage or profitability comes after the basis has become tighter. For entities with these currencies looking to enter new hedges against exchange rate risk for their dollar exposure, it is less expensive and more cost-effective to implement those hedges after the basis has become tighter or more positive. In this case, the profitable trade is to borrow in the high-interest rate currency (the one with a positive basis, i.e. AUD) and lend in a lower interest currency (i.e. US dollar), with exposure to foreign exchange risk well hedged. Borrowers of the US dollar can also borrow more cheaply by first borrowing in the currency of a positive basis and swapping to US dollars while the basis of this currency is still mostly positive.

## 5. Conclusion

This paper establishes the existence, nature, and extent of interconnectedness among the cross-currency basis swap spreads of the major 25 world currencies (G-25). We examine the strength of interconnections and degree of contagion based on the concept of financial networks, a method which is new in the study of linkages in the currency derivatives market. This generates a novel network of assessing the linkages of the G-25 cross-currency swap spreads and examines how the networks of linkages have evolved over different periods.

Our result shows strong evidence of interconnectedness among deviations from the covered interest parity for the currencies both in the tranquil period and during the crisis and post-crisis periods (when the deviations became enlarged). We show that during crisis periods (when markets are more vulnerable), the degree of interconnectedness is particularly stronger and more persistent, which implies mark-to-market losses for investors already with long basis exposures. The systematic and persistent increase in interconnectedness among the cross-currency basis creates larger arbitrage opportunities across the currency and fixed income market for investors with US dollars seeking new positions to raise foreign currencies more cheaply by issuing in US dollars and swapping to the foreign currencies via cross-currency swaps. We also find that the level of derivatives market turmoil and magnitude of interconnectedness recorded their historic highest spikes during the global financial crisis and

the recent coronavirus pandemic than during the eurozone crisis, suggesting stronger evidence of contagion in the cross-currency basis swap markets during the global financial crisis and the recent COVID-19 pandemic. Central to the CIP interconnectedness is the finding that most of the spillovers propagate from the Euro, the Swiss franc, and the Danish krone bases to the other major currencies. Interestingly, the Swiss franc and the Danish krone are pegged closely to the Euro, ultimately making the most influential basis euro-centered, and the main currency that chiefly drives contagion among the bases a Euro play.

It is important to note that we do not directly measure and differentiate the various drivers of the transmission or propagation mechanisms of the potential interconnectedness, or contagion across the cross-currency basis swap spreads analyzed in this paper. As noted in [Forbes and Rigobon \(2002\)](#), directly and exhaustively measuring the various transmission mechanisms of interconnectedness or contagion is an extremely difficult exercise, so we leave that for future research work.

## References

- Acemoglu, D., A. Ozdaglar, and A. Tahbaz-Salehi (2015). Systemic Risk and Stability in Financial Networks. *American Economic Review* 105(2), 564–608.
- Ahelegbey, D. F., M. Billio, and R. Casarin (2016a). Bayesian Graphical Models for Structural Vector Autoregressive Processes. *Journal of Applied Econometrics* 31(2), 357–386.
- Ahelegbey, D. F., M. Billio, and R. Casarin (2016b). Sparse Graphical Vector Autoregression: A Bayesian Approach. *Annals of Economics and Statistics* 123/124, 333–361.
- Ahelegbey, D. F. and P. Giudici (2020). Market Risk, Connectedness and Turbulence: A Comparison of 21st Century Financial Crises. *SSRN 3584510 (accessed on August 9, 2020)*.
- Aizenman, J. and G. K. Pasricha (2010). Selective Swap Arrangements and the Global Financial Crisis: Analysis and Interpretation. *International Review of Economics & Finance* 19(3), 353–365.
- Allen, F. and D. Gale (2000). Financial Contagion. *Journal of Political Economy* 108(1), 1–33.
- Avdjiev, S., W. Du, C. Koch, and H. S. Shin (2019). The Dollar, Bank Leverage, and Deviations from Covered Interest Parity. *American Economic Review: Insights* 1(2), 193–208.
- Avdjiev, S., E. Eren, and P. McGuire (2020). Dollar Funding Costs During the Covid-19 Crisis Through the Lens of the FX Swap Market. Technical report, Bank for International Settlements.
- Avdjiev, S., P. Giudici, and A. Spelta (2019). Measuring Contagion Risk In International Banking. *Journal of Financial Stability* 42, 36–51.
- Baba, N., R. N. McCauley, and S. Ramaswamy (2009). US Dollar Money Market Funds and Non-US Banks. *BIS Quarterly Review, March*.
- Baba, N. and F. Packer (2009a). From Turmoil to Crisis: Dislocations in the FX Swap Market Before and After the Failure of Lehman Brothers. *Journal of International Money and Finance* 28(8), 1350–1374.
- Baba, N. and F. Packer (2009b). Interpreting Deviations from Covered Interest Parity During the Financial Market Turmoil of 2007–08. *Journal of Banking and Finance* 33(11), 1953–1962.
- Baba, N., F. Packer, and T. Nagano (2008). The Spillover of Money Market Turbulence to FX Swap and Cross-Currency Swap Markets. *BIS Quarterly Review, March*.
- Barigozzi, M. and C. Brownlees (2019). NETS: Network Estimation for Time Series. *Journal of Applied Econometrics* 34(3), 347–364.
- Barigozzi, M. and M. Hallin (2017). A Network Analysis of the Volatility of High-Dimensional Financial Series. *Journal of the Royal Statistical Society: Series C (Applied Statistics)* 66(3), 581–605.
- Basu, S. and G. Michailidis (2015). Regularized Estimation in Sparse High-dimensional Time Series Models. *The Annals of Statistics* 43(4), 1535–1567.
- Billio, M., R. Casarin, and L. Rossini (2019). Bayesian Nonparametric Sparse VAR Models. *Journal of Econometrics* 212(1), 97–115.
- Billio, M., M. Getmansky, A. W. Lo, and L. Pelizzon (2012). Econometric Measures of Connectedness and Systemic Risk in the Finance and Insurance Sectors. *Journal of Financial Economics* 104(3), 535 – 559.
- Blume, L., D. Easley, J. Kleinberg, R. Kleinberg, and É. Tardos (2013). Network Formation in the Presence of Contagious Risk. *ACM Transactions on Economics and Computation* 1(2), 6.

- Callier, P. (1981). One Way Arbitrage, Foreign Exchange and Securities Markets: A Note. *The Journal of Finance* 36(5), 1177–1186.
- Cerutti, E. M., M. Obstfeld, and H. Zhou (2019). Covered Interest Parity Deviations: Macrofinancial Determinants. Technical report, National Bureau of Economic Research.
- Coffey, N., W. B. Hrungr, and A. Sarkar (2009). Capital Constraints, Counterparty Risk, and Deviations from Covered Interest Rate Parity. *Federal Reserve Bank of New York Staff Reports* 393.
- Diebold, F. X. and K. Yilmaz (2014). On the Network Topology of Variance Decompositions: Measuring the Connectedness of Financial Firms. *Journal of Econometrics* 182(1), 119–134.
- Du, W. and J. Schreger (2016). Local Currency Sovereign Risk. *The Journal of Finance* 71(3), 1027–1070.
- Du, W., A. Tepper, and A. Verdelhan (2018). Deviations from Covered Interest Rate Parity. *The Journal of Finance* 73(3), 915–957.
- Fong, W.-M., G. Valente, and J. K. Fung (2010). Covered Interest Arbitrage Profits: The Role of Liquidity and Credit Risk. *Journal of Banking and Finance* 34(5), 1098–1107.
- Forbes, K. J. and R. Rigobon (2002). No Contagion, Only Interdependence: Measuring Stock Market Comovements. *The Journal of Finance* 57(5), 2223–2261.
- Freixas, X., B. M. Parigi, and J.-C. Rochet (2000). Systemic Risk, Interbank Relations, and Liquidity Provision by the Central Bank. *Journal of Money, Credit and Banking* 32(3), 611–638.
- Geiger, D. and D. Heckerman (2002). Parameter Priors for Directed Acyclic Graphical Models and the Characterization of Several Probability Distributions. *Annals of Statistics* 30(5), 1412–1440.
- Gelman, A. and D. B. Rubin (1992). Inference from Iterative Simulation Using Multiple Sequences, (with discussion). *Statistical Science* 7, 457–511.
- George, E. I., D. Sun, and S. Ni (2008). Bayesian Stochastic Search for VAR Model Restrictions. *Journal of Econometrics* 142, 553–580.
- Goldberg, L. S., C. Kennedy, and J. Miu (2011). Central Bank Dollar Swap Lines and Overseas Dollar Funding Costs. *Federal Reserve Bank of New York Economic Policy Review*, 3–20.
- Haldane, A. G. (2013). Rethinking The Financial Network. In *Fragile Stabilität–Stabile Fragilität*, pp. 243–278. Springer.
- Hui, C.-H., H. Genberg, and T.-K. Chung (2011). Funding Liquidity Risk and Deviations from Interest-Rate Parity During the Financial Crisis of 2007-2009. *International Journal of Finance and Economics* 16(4), 307–323.
- Ibhagui, O. (2019). Interrelations among Cross-Currency Basis Swap Spreads: Pre-and Post-crisis Analysis. *The Journal of Derivatives* 26(4), 89–112.
- Kritzman, M. and Y. Li (2010). Skulls, Financial Turbulence, and Risk Management. *Financial Analysts Journal* 66(5), 30–41.
- Roberts, G. O. and S. K. Sahu (1997). Updating Schemes, Covariance Structure, Blocking and Parametrization for the Gibbs Sampler. *Journal of the Royal Statistical Society* 59, 291 – 318.
- Shleifer, A. and R. W. Vishny (1997). The Limits of Arbitrage. *The Journal of Finance* 52(1), 35–55.

## Appendix A. Network Sampling Algorithm

This section provides a detailed description of the sampling approach of the networks. Given some lag length  $\hat{p}$ , inference of the network is made feasible by integrating out other parameters analytically to obtain a marginal likelihood function over graphs (see [Ahelegbey et al., 2016a](#); [Geiger and Heckerman, 2002](#)). Let  $V_y = (y_i, \dots, y_n)$  be the vector of indices of response variables, and  $V_z = (z_1, \dots, z_{n\hat{p}})$  the indices of the variables in  $Z$ . The network relationship from  $z_\psi \in V_z$  to  $y_i \in V_y$  can be represented by ( $G_{y_i, z_\psi} = 1$ ). Following [Geiger and Heckerman \(2002\)](#), the closed-form expression of the local marginal likelihood is given by

$$P(Y|G_{y_i, z_\psi}) = \frac{\pi^{-\frac{1}{2}N} \nu_0^{\frac{1}{2}\nu_0} \Gamma(\frac{\nu_0 + N - n_x}{2})}{\nu_n^{\frac{1}{2}\nu_n} \Gamma(\frac{\nu_0 - n_x}{2})} \left( \frac{|Z'_\psi Z_\psi + \nu_0 I_{n_\psi}|}{|X'_i X_i + \nu_0 I_{n_x}|} \right)^{\frac{1}{2}\nu_n} \quad (\text{A.1})$$

where  $\Gamma(\cdot)$  is the gamma function,  $X_i = (Y_i, Z_\psi)$ ,  $I_d$  is a  $d$ -dimensional identity matrix,  $n_\psi$  is the number of covariates in  $Z_\psi$ ,  $n_x = n_\psi + 1$ ,  $\nu_0 > n_x$  is a degree of freedom hyper-parameter of the prior precision matrix of  $(Y, Z)$ , and  $\nu_n = \nu_0 + N$ .

Algorithms 1 and 2 samples  $[G_{1:\hat{p}}|Y, \hat{p}]$  and  $[G_0|Y, \hat{G}_{1:\hat{p}}, \hat{p}]$ , respectively, via a Metropolis-within-Gibbs scheme with random walk proposal. In a typical MCMC algorithm, the space exploration crucially depends on the choice of the starting point of the chain. Usually, a set of burn-in iteration is advanced to obtain a good starting point. We navigate around this problem by initializing the network search with a Granger-causality-like structure. More precisely, we examine if the prediction of a response variable can be improved by incorporating information from each of the explanatory variables. The set of variables that pass this test are retained to provide a starting structure for the MCMC iteration, which is designed to sample the combination of explanatory variables that produce high-scoring networks.

---

**Algorithm 1** Sampling  $[G_{1:\hat{p}}|Y, \hat{p}]$

---

- 1: **Require:** Set of responses  $V_y = (y_1, \dots, y_n)$  and lagged attributes  $V_z = (z_1, \dots, z_{n\hat{p}})$
  - 2: Initialize  $G_{1:\hat{p}}^{(1)} = \emptyset$
  - 3: **for**  $y_i \in V_y$  **do**
  - 4:     **for**  $z_j \in V_z$  **do**
  - 5:         Compute  $\phi_a = P(Y|G_{y_i, \emptyset|1:\hat{p}}^{(1)})$  and  $\phi_b = P(Y|G_{y_i, z_j|1:\hat{p}}^{(1)})$
  - 6:         **if**  $\phi_b > \phi_a$  **then**  $G_{y_i, z_j|1:\hat{p}}^{(1)} = 1$  **else**  $G_{y_i, z_j|1:\hat{p}}^{(1)} = 0$
  - 7: **for**  $h = 2 : H$ , (MCMC Iteration by performing local network update) **do**
  - 8:     **for**  $y_i \in V_y$ , set  $G_{y_i|1:\hat{p}}^{(*)} = G_{y_i|1:\hat{p}}^{(h-1)}$  **do**
  - 9:         Randomly draw  $z_k \sim V_z$
  - 10:         Add/remove link from  $z_k$  to  $y_i$ :  $G_{y_i, z_k|1:\hat{p}}^{(*)} = 1 - G_{y_i, z_k|1:\hat{p}}^{(h-1)}$
  - 11:         Compute  $\phi = \exp [ \log P(Y|G_{y_i|1:\hat{p}}^{(*)}) - \log P(Y|G_{y_i|1:\hat{p}}^{(h-1)}) ]$ . Draw  $u \sim \mathcal{U}(0, 1)$ .
  - 12:         **if**  $u < \min\{1, \phi\}$  **then**  $G_{y_i|1:\hat{p}}^{(h)} = G_{y_i|1:\hat{p}}^{(*)}$  **else**  $G_{y_i|1:\hat{p}}^{(h)} = G_{y_i|1:\hat{p}}^{(h-1)}$
- 

---

**Algorithm 2** Sampling  $[G_0|Y, \hat{G}_{1:\hat{p}}, \hat{p}]$

---

- 1: **Require:** Set of attributes  $V_y = (y_1, \dots, y_n)$  and estimated lag network  $\hat{G}_{1:\hat{p}}$
  - 2: Initialize  $G_0^{(1)} = \emptyset$  and  $G_{0:\hat{p}}^{(1)} = [G_0^{(1)}, \hat{G}_{1:\hat{p}}]$
  - 3: **for**  $y_i \in V_y$  **do**
  - 4:     Set  $V_{y_i} = V_y \setminus \{y_i\}$  and  $\{z_\pi : \hat{G}_{y_i, z_\pi|1:\hat{p}} = 1\}$
  - 5:     **for**  $y_j \in V_{y_i}$  **do**
  - 6:         Set  $\pi_i = (y_j \cup z_\pi)$ . Compute  $\phi_a = P(Y|G_{y_i, z_\pi|0:\hat{p}}^{(1)})$  and  $\phi_b = P(Y|G_{y_i, \pi_i|0:\hat{p}}^{(1)})$
  - 7:         **if**  $\phi_b > \phi_a$  **then**  $G_{y_i, \pi_i|0:\hat{p}}^{(1)} = 1$  **else**  $G_{y_i, z_\pi|0:\hat{p}}^{(1)} = 1$
  - 8: **for**  $h = 2 : H$ , (MCMC Iteration by performing local network update) **do**
  - 9:     **for**  $y_i \in V_y$ , set  $G_{y_i|0:\hat{p}}^{(*)} = G_{y_i|0:\hat{p}}^{(h-1)}$  **do**
  - 10:         Randomly draw  $y_k \sim V_{y_i}$
  - 11:         Add/remove link from  $y_k$  to  $y_i$ :  $G_{y_i, y_k|0:\hat{p}}^{(*)} = 1 - G_{y_i, y_k|0:\hat{p}}^{(h-1)}$
  - 12:         Compute  $\phi = \exp [ \log P(Y|G_{y_i|0:\hat{p}}^{(*)}) - \log P(Y|G_{y_i|0:\hat{p}}^{(h-1)}) ]$ . Draw  $u \sim \mathcal{U}(0, 1)$ .
  - 13:         **if**  $u < \min\{1, \phi\}$  **then**  $G_{y_i|0:\hat{p}}^{(h)} = G_{y_i|0:\hat{p}}^{(*)}$  **else**  $G_{y_i|0:\hat{p}}^{(h)} = G_{y_i|0:\hat{p}}^{(h-1)}$
-

*Appendix A.1. Convergence and Mixing of MCMC*

We examine the mixing of the chains generated by the Gibbs sampler for the samples of  $G = \{G_{1:p}, G_0\}$ . We monitor the mixing of the MCMC by computing the local log-likelihood score. We use the score to compute the potential scale reduction factor (PSRF) and multivariate PSRF (MPSRF) of [Gelman and Rubin \(1992\)](#). Following standard application, the MCMC chain is considered as converged if the PSRF and MPSRF are less than 1.2. With 50,000 sampled networks, we ensure that the convergence and mixing of the MCMC chains are tested with both PSRF and MPSRF satisfying the above condition.

We estimate the posterior probability of the edges by averaging over the sampled networks, i.e.,  $\hat{\gamma}_{ij} = \frac{1}{H} \sum_{h=1}^H G_{i,j}^{(h)}$ , where  $H$  is the total number of posterior samples of the graph. Due to the uncertainty in the network link determination, we consider a one-sided posterior credibility interval for the edge posterior distribution. Following [Ahelegbey et al. \(2016a\)](#), we parameterize the  $ij$ -th entry of the estimate of  $\hat{G}$  via a link function:

$$\hat{G}_{i,j} = \mathbf{1}(q_{ij} > 0.5), \quad q_{ij} = \hat{\gamma}_{ij} - z_{(1-\alpha)} \sqrt{\frac{\hat{\gamma}_{ij}(1 - \hat{\gamma}_{ij})}{n_{\text{eff}}}}, \quad n_{\text{eff}} = \frac{H}{1 + 2 \sum_{t=1}^{\infty} \rho_t} \quad (\text{A.2})$$

where  $n_{\text{eff}}$  is the MCMC effective sample size of the network graph,  $\rho_t$  is the autocorrelation of the graph scores at lag  $t$ , and  $z_{(1-\alpha)}$  is the z-score of the normal distribution at  $(1 - \alpha)$  significance level. A default value for  $\alpha$  is 0.05 and  $z_{(1-\alpha)} = 1.65$ .